Energy Based Performance Evaluation of Passive EPC Gen 2 Class 1 RFID Systems

Farzad Hessar, *Student, IEEE*, and Sumit Roy, *Fellow, IEEE*

***Abstract*—This paper analyzes performance of RFID networks that are based on passive tags using EPC Gen2 Class1 communication protocol. For the first time, all the main factors impacting tag read efficiency and read latency are considered - inclusive of MAC layer collision, link layer packet loss and the impact of the use of energy harvesting in passive tags. Specifically, the impact of tag duty cycling due to limited harvested energy is considered - a first in the analysis of RFID systems, to the best of our knowledge.**

***Index Terms*—RFID, MAC, slotted ALOHA, EPC, energy harvesting, cross layer.**

I. Introduction

RADIO Frequency Identification technology employs radio frequency (RF) communication to store and retrieve data on-tag through an RF compatible integrated circuit. In the past few years, RFID has increasingly been found in everyday applications, ranging from inventory control, vehicle tracking to electronic tolling and card-reading, mainly because of its cost efficiency proposition. The main components of an RFID system are: a *reader* (interrogator) that initiates read/write of data to/from RFID tags; and a *tag* (transponder) that contains information about the object it is affixed to. RFID provides (potentially) a more efficient and inexpensive mechanism for automatically collecting and updating information regarding a tagged object, as compared to the optical bar-code scanning technology it is intended to replace.

Depending on the application, different types of tags may be used. *Active/semi-passive* tags contain an embedded power source and a CPU which enables stand alone processing. On the other hand, passive tags do not have a power supply and must harvest energy from RF downlink carrier sent from the reader. Low maintenance cost (no replacing batteries) and improved device life time make passive tags an attractive choice for many applications, however, their communication and computation capabilities are limited.

An RFID reader attempts to read all tags (each attached to an object) that are present within its read range. In this work, we analyze the achievable read rates, which are impacted by a number of factors, namely:

- *Tag Collision*: Since all tags share a common uplink, multiple transmissions may lead to collision and packet loss. The EPC Gen2 Class 1 protocol [1] utilizes a modified version of Framed Slotted ALOHA at the MAC layer for anti-collision. The probability of collision is sensitive to the choice of the frame size, whose optimum setting depends on the number of responding tags (which is generally unknown).
- *Link Failure*: In the absence of collision, tag packets may also be lost due to channel noise since the signal-to-noise ratio at the reader input is often low.
- *Power Limitation*: Passive tags receive all their energy from harvesting. Harvested energy/power is a function of distance from reader (r) and decreases according to a power law with exponent of 2 or higher. *At typical separations, the average harvested power is usually less than that required by the tag circuitry for continuous operation*. As a result, tag must switch to sleep mode, harvest energy and then return to normal operation. This duty cycling greatly affects the read rate as shown in our performance analysis.

A comprehensive study of performance analysis should consider all three factors above because they are inter-related with each other. For example, because of power limitations and resulting duty cycling, tag is 'on' for just a limited time interval of length T_{on} before switching to standby mode. As we will prove later, the average number of *successful* queries that occurs during the interval T_{on} is not a linear function of the duration (not proportional to T_{on}). Moreover, unlike traditional ALOHA based protocols, EPC G2C1 utilizes shorter slots for *collided/empty/invalid ACK* compared to *successful* query rounds. Therefore, a link failure due to channel noise can turn a *successful* query to *unsuccessful* which has a different duration and thus changes effective number of query rounds over the interval T_{on}. Hence, a *cross layer performance analysis that is energy-aware* is desirable which models core aspects of the MAC and PHY layer simultaneously. This has largely not occurred to-date; a significant portion of the RFID performance analysis literature focuses exclusively on the tag collision aspect of the MAC protocol [2]–[8] (and its consequent amelioration) but without integrating it into a broader analysis of read rates. MAC-PHY interactions is mentioned in [9] but the performance evaluation is limited to only the physical layer. An energy based approach was attempted in [10]–[13] but it did not include a model for tag power harvesting. Our approach thus leads to a much more realistic estimate of maximum achievable tag read rate in practice, as compared to prior analytical approaches.

Section 2 introduces a block diagram for the various energy states of a tag as well as an energy model. Section 3 models the tag as a finite state machine for the various processing

Manuscript received September 7, 2011; revised July 15 and December 19, 2012. The associate editor coordinating the review of this letter and approving it for publication was F. Santucci.

F. Hessar (corresponding author) and S. Roy are with the Department of Electrical Engineering, University of Washington, Seattle 98195, WA (e-mail: {farzad, sroy}@u.washington.edu).

Digital Object Identifier 10.1109/TCOMM.2013.13.110603

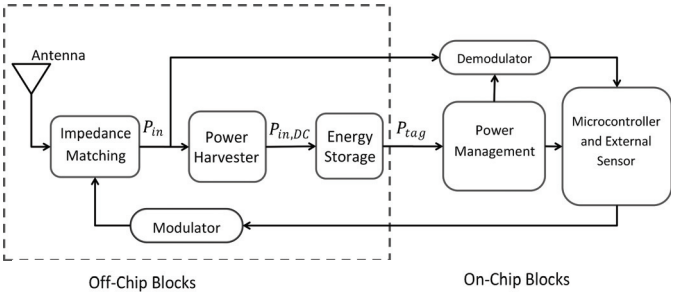

Fig. 1. A typical block diagram for passive tags.

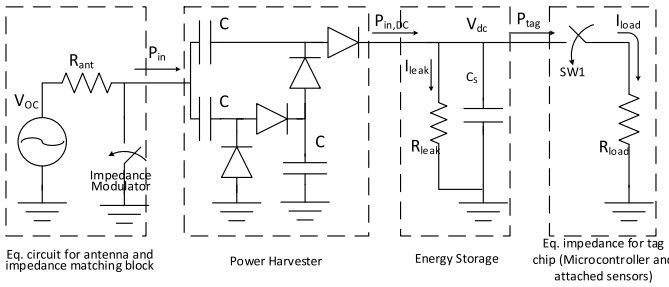

Fig. 2. Equivalent circuit diagram for passive tags according to Fig. 1. Impedance matching block is considered in antenna eq. circuit and R_{load} models the tag chip (including Micro-controller and attached sensors).

functions in support of back-scatter communications. Section 4 introduces MAC Layer of EPC Gen2. Section 5 develops MAC Layer performance analysis (in terms of tag read rate) based on aforementioned model. Section 6 presents simulation results of tag performance to validate the theoretical predictions and explores effects of system parameters variations. Finally, Section 7 concludes the paper.

II. Energy Model

Energy harvesting and consumption in passive RFID tags is strongly dependent on the relevant circuit designs. Fig. 1 shows a typical block diagram for a tag highlighting the following main components:

- Impedance matching circuit that controls input impedance (usually input resistance) which in turn determines the input power absorbed from antenna (P_{in} in Fig. 1) on the downlink. Here we assume that input impedance is switched between one of the two states: a) either $Z_{in} = 0$ (leads to no absorbed power) or b) $Z_{in} = Z^*_{ant}$ (for maximum absorbed power) where Z_{ant} is antenna impedance.
- Power harvester block converts the input power P_{in} from ac to dc voltage V_{dc} which is stored inside the energy storage capacitor C_S. The stored energy E_{std} (or equivalent voltage level V_{dc}, $E_{std} = \frac{C_S V_{dc}^2}{2}$) is the only energy source available to the tag for all operations by its micro-controller.
- The micro-controller is the processing unit which conducts all the necessary on-tag processing: backscatter communication (via EPC state machine), data reads from any integrated on-tag sensor, read/write from tag memory, etc.
- Power Management Block (PMB) is the energy supervisor; it monitors the capacitor voltage and provides input for decisions regarding tag operations. PMB utilizes two voltage thresholds V_L(low) and V_H (high); if $V_{dc} < V_L$, the tag enters standby mode with minimal power consumption so as to begin recovery of the voltage level back to operating threshold value V_H for normal operation. The lower threshold V_L is chosen according to minimum required dc voltage for digital circuits. The purpose of utilizing V_H is to ensure V_{dc} does not fall below V_L immediately after returning back from standby mode.

A. Specification of Power Harvester Block

A common RF to DC converter circuit used for power harvesting is the Dickson charge pump, even though the circuit was originally designed for rectangular pulses and not RF carriers. It consists of diodes for rectification of voltage and capacitors for preserving the voltage envelope level. A number of these charge pumps are required for amplification to achieve the target voltage level for normal IC operation. A two stage charge pump equivalent circuit is shown in Fig. 2 with the antenna radiation resistance R_{ant} and open circuit voltage V_{OC}. The capacitor C_S is sufficiently large and holds the stored energy. R_{leak} models the leakage current and R_{load} is the tag chip impedance. Using the well-known Friis equation for free space, the input power P_{in} at the tag antenna and the corresponding open circuit voltage V_{OC} in terms of *transmitted power* by the reader P_T and reader-tag distance r is given by

$$V_{OC} = 2\sqrt{2R_{ant}P_{in}} \tag{1}$$

$$P_{in} = P_T \left(\frac{\lambda}{4\pi r}\right)^2 \gamma G_T G_R L_P \tag{2}$$

where λ is carrier wavelength, G_T, G_R, L_P are the tag/reader antenna gains, and all losses (such as due to polarization loss), respectively. γ is slow-fading factor that is assumed to be constant over transmission time for reading tag's data by interrogator.

The switch SW1 in Fig. 2 models the tag's operational status (normal/standby) - it is open for standby mode but closed for normal operation allowing load current I_{load} to flow through R_{load}. The rectified voltage V_{dc} in steady state is described in terms of V_{OC}, number of charge pump stages N and I_{load} as [14]–[18]

$$V_{dc} = 2N(V_{OC} - V_t) - \left(\frac{2N}{f_c C} + 8 * 2^N R_{ant}\right)(I_{load} + I_{leak}) \tag{3}$$

where V_t is the turn-on threshold voltage for rectifying diodes and f_c is the carrier frequency. The term $8 * 2^N R_{ant}$ is the equivalent resistant to R_{ant} that is seen from the output. Every multiplier stage doubles the impedance which results in $2^N R_{ant}$ for N stages. The coefficient 8 is found through circuit simulation in PSPICE for various situations and loads. This increase in impedance is mainly because the input signal is a sine wave rather than pulse waves and therefore within every RF interval of length $T_c = \frac{1}{f_c}$ diodes remains off until

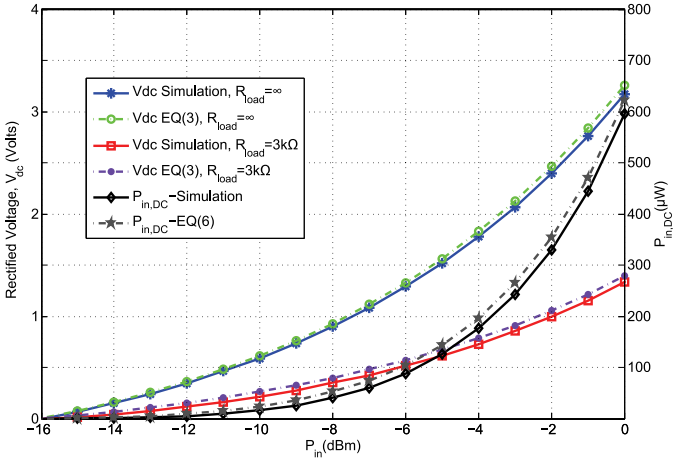

Fig. 3. Rectified voltage and dc power v.s. input power for $N = 5$.

the input voltage crosses the threshold V_t which is a significant portion of the period. For low frequency applications of Dickson circuit, $\frac{2N}{f_c C} >> 2^{N+3} R_{ant}$ and the latter term is usually ignored. For example in HF RFID, for $C = 1$pF, $R_{ant} = 50\Omega$, $f_c = 13.6$MHz and $N = 5$, the first term is more than 50 times larger than the second term.

For a fixed input power P_{in} and N, the maximum rectified voltage $V_{dc,max}$ is achieved by letting $I_{load} = 0$ (standby mode, SW1 is open). This can be used for finding the maximum operational range of the down link. Since the minimum acceptable voltage is V_L, then from (1)-(3), the maximum distance $r_{max,dlink}$ for successfully decoding the down link is

$$r_{max,dlink} = \frac{\lambda}{2\pi} \frac{\sqrt{2R_{ant} P_T \gamma G_T G_R L_P}}{\frac{V_L}{2N} + V_t + I_{leak}(\frac{1}{f_c C} + \frac{2^{N+3} R_{ant}}{2N})} \quad (4)$$

Note that if $r > r_{max,dlink}$ then $V_{dc,max}$ drops below V_L and tag never turns on.

The use of non-ideal diodes as rectifiers ($V_t \neq 0$) not only decreases the rectified voltage, it also decreases the dc power delivered to an external load. The resulting efficiency of rectification is well approximated [14] by

$$\eta_{rect}(V_{dc}) = \frac{V_{dc}}{V_{dc} + 2NV_t} \quad (5)$$

which suggests that the efficiency could be dramatically low when V_{dc} (or equivalently P_{in}) is small. The effective dc power delivered to storage unit and R_{load} is therefore

$$P_{in,DC}(V_{dc}) = P_{in} \times \eta_{rect}(V_{dc}) \quad (6)$$

Fig. 3 shows the rectified voltage in (1)-(3) for both *Standby* mode ($R_{load} = \infty$) and *Active* mode ($R_{load} = 3k\Omega$) against PSPICE simulation of the Dickson pump. The parameters for the U Washington WISP tag [19] were obtained from the design team, i.e., $V_t = 0.1$,$R_{ant} = 50\Omega$, $f_c = 900MHz$, $C = 10pF$, $N = 5$. The figure also shows the rectified dc power $P_{in,DC}$ as in (6) together with corresponding circuit simulation. Increasing the input power P_{in} results in a higher rectified dc voltage V_{dc} which in turn leads to higher rectification efficiency as in (5). Therefore, harvested power increases rapidly as P_{in} increases.

B. Harvesting cycles

The output voltage of harvester block drops below $V_{dc,max}$ as PMB closes SW1 (when normal tag operation starts and the tag chip starts draining power from storage C_S). The dc power taken from C_S is sum of the tag chip power $P_{tag}(V_{dc}) = \frac{V_{dc}^2}{R_{load}}$ and leakage power $P_{leak}(V_{dc}) = \frac{V_{dc}^2}{R_{leak}}$. Depending on the load factor $\frac{P_{tag}(V_L)+P_{leak}(V_L)}{P_{in,DC}(V_L)}$, the output voltage behaves differently. Two possible cases are:

- $P_{tag}(V_L) + P_{leak}(V_L) \leq P_{in,DC}(V_L)$: Rectified power $P_{in,DC}$ is enough to provide for total dissipated power $(P_{tag}(V_L) + P_{leak}(V_L))$ at minimum allowed voltage V_L. The rectified voltage, in this case, drops from un-loaded voltage $V_{dc,max}$ but it never goes below V_L. This allows the tag to run continuously and PMB never places the tag in standby mode, hence the duty cycle is unity.
- $P_{tag}(V_L) + P_{leak}(V_L) > P_{in,DC}(V_L)$: The input power does not suffice to keep the tag running continuously. Rectified voltage V_{dc} decreases over time until it reaches V_L and PMB places the tag into standby. Rectified voltage starts increasing in the standby mode upto V_H. A harvesting cycle is defined as an interval of length T over which rectified voltage drops from V_H to V_L and then increases back to V_H. Tag behavior in this case is cyclical with net period T, including an 'on' interval of length T_{on} in which tag is in normal operation (able to communicate to reader) and an 'off' interval of length T_{off} in which it is only harvesting energy; i.e., $T = T_{\text{on}} + T_{\text{off}}$.

The duration of 'on'/'off' cycles is determined by charge / discharge patterns of capacitors in Dickson pump. There exists no closed form equation that describes the charge/discharge behavior in terms of circuit components and input power. The non-linear behavior of rectifying diodes make analysis difficult. Thus, simulation of the rectifier circuit in Fig. 2 was conducted via PSPICE/ORCAD [20], which reveals that a first order R-C circuit approximation for both charge and discharge intervals is a reasonable approximation. Hence:

1) Charge interval: The transient voltage has the following exponential form during the standby mode

$$V_{dc,\text{off}}(t) = (V_{0,\text{off}} - V_{\infty,\text{off}})e^{-t/\tau_{\text{off}}} + V_{\infty,\text{off}} \quad (7)$$

where $V_{0,\text{off}} = V_L$ is the initial voltage at the time of switching from normal to standby, $V_{\infty,\text{off}}$ is the steady state voltage and τ_{off} is the time constant of the circuit in standby mode. The steady state voltage is achieved from (3) by setting $I_{load} = 0$,

$$V_{\infty,\text{off}} = 2N(V_{OC} - V_t) - (\frac{2N}{f_c C} + 2^{N+3} R_{ant}) I_{leak} \quad (8)$$

Determination of τ_{off} needs an exact investigation of energy harvesting procedure happening in the Dickson circuit. The input carrier charges the internal capacitors C during each period of length $T_c = \frac{1}{f_c}$ with a time constant proportional to $2NR_{ant}C$. With an additional assumption of $R_{ant}C << T_c$, all R-C charging between R_{ant} and all $2N$ capacitors C reach their steady state. The input

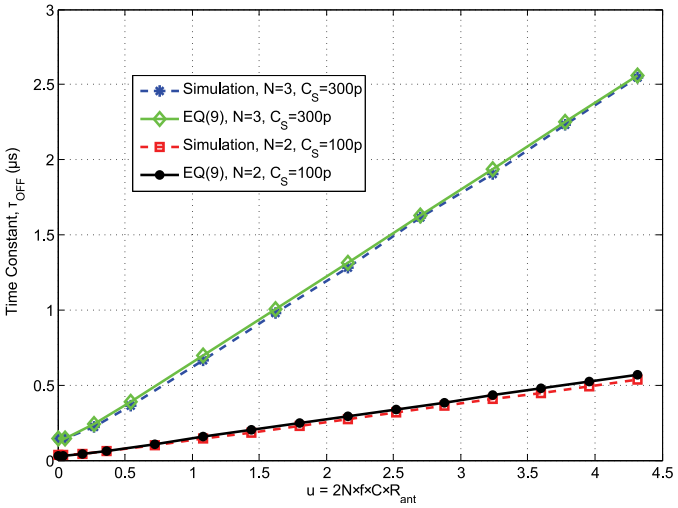

Fig. 4. Simulation of time constant for Dickson circuit with two different set of parameters. Circuit simulation is performed in PSPICE with $C_S = 100/300pF$, $C = 10pF$, $N = 2/3$, $f_c = 900MHz$.

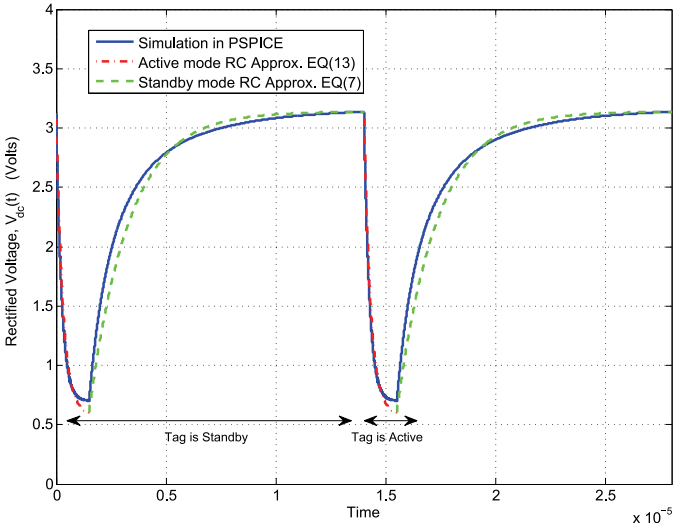

Fig. 5. Simulation of transient behavior of harvester circuit and comparison with theoretical approximations (7)-(14). Circuit simulation is performed in PSPICE with $R_{load} = 1k\Omega$, $C_S = 300pF$, $C = 10pF$, $N = 3$, $f_c = 900MHz$, $V_t = 0.1$.

must pass through all $2N$ internal capacitors until it begins to charge C_S. Also, since the storage capacitor $C_S >> C$ it requires $\frac{C_S}{C}$ times more time to charge it to the same voltage as C. By performing circuit simulation of Dickson circuit in PSPICE and exponential curve-fitting algorithms in MATLAB [20], the net time constant of the harvester circuit is found to be well approximated as $\tau_{\text{off}} = 0.8 \times \frac{2NC_S/C}{f_c}$. The simplifying assumption of $R_{ant}Cf_c << 1$ is usually met in HF application of RFID and not in UHF RFID tags, $N = 5, C = 10pF, f_c =$ 900MHz, $R_{ant} = 50\Omega \rightarrow 2NR_{ant}f_cC = 4.5 \not< 1$. In this case, internal capacitors presents exponential voltage increase during T_c interval and they decrease the overall time constant of the circuit to

$$\tau_{\text{off}} = \frac{0.8 \times 2NC_S}{f_cC(1 - \exp(\frac{-1}{8NR_{ant}Cf_c}))} \tag{9}$$

which is verified through circuit simulation [20] for various parameters including C_S, N, R_{ant}. Fig. 4 shows τ_{off} as a function of $u = 2Nf_cCR_{ant}$ for two different set of parameters. As can be seen, analytical results based on (9) follow circuit simulation results precisely.
Using (7)-(9), the required time for restoring voltage from V_L back to V_H is

$$T_{\text{off}} = \tau_{\text{off}} \ln\left(\frac{V_{\infty,\text{off}} - V_L}{V_{\infty,\text{off}} - V_H}\right) \tag{10}$$

2) Discharge interval: While the tag is active, transient response of rectified voltage could still be modeled as in (7). However, in this case, we propose a different approach to estimate the model parameters. By the *Conservation of Energy* principle, the amount of input energy post-rectification over a small interval of dt must equal the a) sum of dissipated energy in $R_{eq} = R_{load}||R_{leak}$ and b) change in energy in the storage capacitor C_S. Hence

$$P_{diss} + \frac{C_S[V^2_{dc,\text{on}}(t+dt) - V^2_{dc,\text{on}}(t)]}{2dt} = \eta_{rect}(V_{dc,\text{on}}(t))P_{in} \tag{11}$$

where $P_{diss} = \frac{V^2_{dc,\text{on}}(t)}{R_{eq}}$ is the dissipated power in R_{eq}. By substituting $\eta_{rect}(V_{dc,\text{on}}(t))$ from (5), we arrive at the following differential equation:

$$V_{dc,\text{on}}(t)[V_{dc,\text{on}}(t) + 2NV_t] - R_{eq}P_{in} = -R_{eq}C_S\acute{V}_{dc,\text{on}}(t)[2NV_t + V_{dc,\text{on}}(t)] \tag{12}$$

By substituting exponential form for $V_{dc,\text{on}}(t) = ae^{-bt}+c$ in the above equation and initial condition of $V_{dc,\text{on}}(0) = V_H$, the transient rectified voltage in active mode is found to be

$$V_{dc,\text{on}}(t) = (V_H - \beta)e^{\frac{-t}{R_{eq}C_S}} + \beta \tag{13}$$

where $\beta = \frac{-2NV_t + \sqrt{(2NV_t)^2 + 4R_{eq}P_{in}}}{2}$. Using this, the duration of active mode is determined by setting $V_{dc,\text{on}}(t) = V_L$,

$$T_{\text{on}} = R_{eq}C_S \ln\left(\frac{V_H - \beta}{V_L - \beta}\right) \tag{14}$$

Fig. 5 provides circuit level simulation of the charge pump in PSPICE as well as first order R-C analysis based on (7)-(14). The R-C approximations follows the simulation results very well and verifies the assumed model.

Note that both (10) and (14) assume *constant* input power from reader which does not account for amplitude modulation on the downlink and backscatter modulation in tag. These effects will be considered in the next section.

III. Tag State Machine

A Gen2 compatible tag may be modeled as a finite state machine with a number of state descriptions governed not only

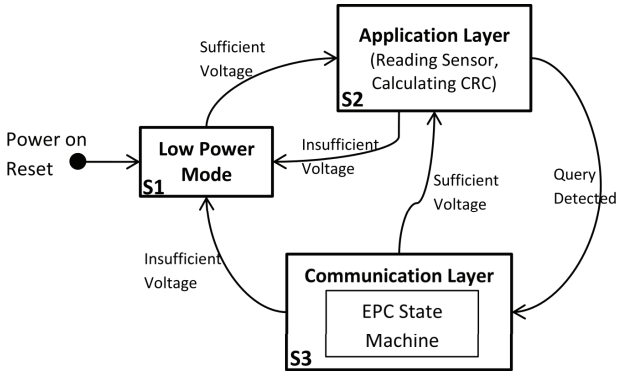

Fig. 6. Typical state transition diagram for passive tags [19].

by the functions being executed on-tag, but also by its energy state. State transitions are based on residual energy as well as reader commands, as shown in Fig. 6. The three major tag states are as follows:

- **S1 - Low Power Mode**: This is a low power state intended for restoring voltage from V_L back to V_H. The micro-controller is in a minimal power consumption mode where it just preserves current status of memory and registers. Because of this, tag controller does not accomplish any other task except waiting for an external interrupt which indicates there is enough energy in the storage capacitor. Therefore, S1 represents the T_{off} subinterval of each cycle; transition into this may happen from any other state, whenever the storage capacitor voltage falls below V_L. Following S1, tag always moves to S2 (application mode).
- **S2 - Application Mode**: This represents 'normal' operation for which tag is designed. For example in the case of a sensor network application, this may include data reads from an on-tag sensor (or other external sensor connected to the tag) and calculating CRC[1] for the newly read data. For supply chain scenarios, this would consist of reading the EPC code (a constant value bit string of length 96 or 128 bits) from tag's memory for backscatter modulation. Following this state, the tag could transit to either S1 or S3, given sufficient stored voltage/energy.
- **S3 - Communication Mode**: This state includes all operations needed for backscatter communications per EPC Gen 2 Class 1 between the tag and reader. Within S3, tag listens to incoming commands, decodes them and takes necessary actions. The tag to reader uplink uses backscattering modulation of the incoming RF carrier, achieved by switching tag antenna impedance between two nominal values: 0 and Z^*_{ant}.

During backscatter modulation, the effective power transferred to the tag is reduced because some of the incident power is reflected back. This reduces P_{in} in (2) to αP_{in} where α is modulation factor. Moreover, α must consider input power reductions due to reader amplitude modulation in the downlink. EPC protocol makes use of PIE(Pulse Interval Encoding) signals for reader-to-tag communication (downlink) and FM0/Miller line coding for tag-to-reader transmission (uplink). Both FM0 and Miller are composed of rectangular pulses with 50% duty cycle for sending data-0/data-1, hence $\alpha_{\text{FM0}} = 0.5$. PIE symbols are also rectangular ASK pulses but with different durations/duty cycles for data-0 and data-1, defined in terms of a *Tari* duration by the specifications. A data-0 symbol in PIE is of $1.0 \times$ Tari length and $1 - \frac{\text{PW}}{\text{Tari}}$ duty cycle, whereas data-1 symbol duration is $1.75 \times$ Tari with $1 - \frac{\text{PW}}{1.75 \times \text{Tari}}$ duty cycle. Assuming equiprobable 0 and 1 symbols, the effective input power reduction due to reader modulation is $\alpha_{\text{PIE}} = (1 - \frac{2\text{PW}}{2.75\text{Tari}})$.

The effective modulation factor α clearly depends on tag/reader status. During S1/S2, tag does not backscatter but reader transmits either a modulated signal for sending commands or an un-modulated signal for listening to tag backscatters. Hence, $\alpha_{S_{1,2}} = (1 + \alpha_{\text{PIE}})/2$ and duration of 'off' subinterval within each cycle must be calculated based on $\alpha_{S_{1,2}} P_{in}$ as in (1),(10). Within S3, it is either tag or reader sending signals which makes $\alpha_{S_3} = (\alpha_{\text{FM0}} + \alpha_{\text{PIE}})/2$.

During T_{on} sub-interval of each cycle, tag could be either in S2 or S3. It moves to S3 only when it detects a Query command issued by reader otherwise it remains in S2 performing application related computations. Precise value of T_{on} depends on fraction of time spent in S2 compared to S3; we use $\alpha_{S_3} P_{in}$ in (14) as a conservative estimate.

IV. EPC MAC Layer

The reader attempts to read the ID from a group of tags (each attached to a separate object) in its vicinity. Since the EPC uplink MAC protocol is distributed, individual tag responses may interfere with each other while replying back to reader commands. Tag responses are synchronized to the reader Query commands and utilize modified framed slotted ALOHA to resolve interference on the uplink. This is based on *Q-Algorithm* in which reader sends a Query command with an integer parameter Q, asking every tag to generate a 16-bits random number (RN16) uniformly and to mask Q bits of the generated RN16 to form their slot counter. Tags respond with their RN16 when their counter counts down to 0, forming a framed slotted ALOHA multi-access system over a duration of 2^Q slots.

Fig. 7 shows the EPC MAC flowchart corresponding to the transponder actions. Upon power up, tag moves to "Ready" state, waiting for Query command. After receiving a Query command with valid flags[2], it generates RN16 and its slot counter initialization. If slot counter is zero, the tag backscatters RN16, otherwise it goes to "Arbitrate" state. If the reader receives no response or multiple collided responses from several tags, then it sends QueryRep command in response of which tags count down slot counter until they reach zero and reply back (in "Reply" state).

An inventory round is a sequence of consecutive commands and responses that are issued by the reader and replied back by the tag in order to transmit the tag ID (XPC/EPC packet) to the reader. Every round starts with a Query/QueryRep command which asks the tag with zero SC (Slot Counter)

[1]Cyclic Redundancy Check

[2]Query commands consist of specific flags which enable the reader to inventory a specific tag population. These flags are programmable within EPC to prevent individual tag from multiple unnecessary responses.

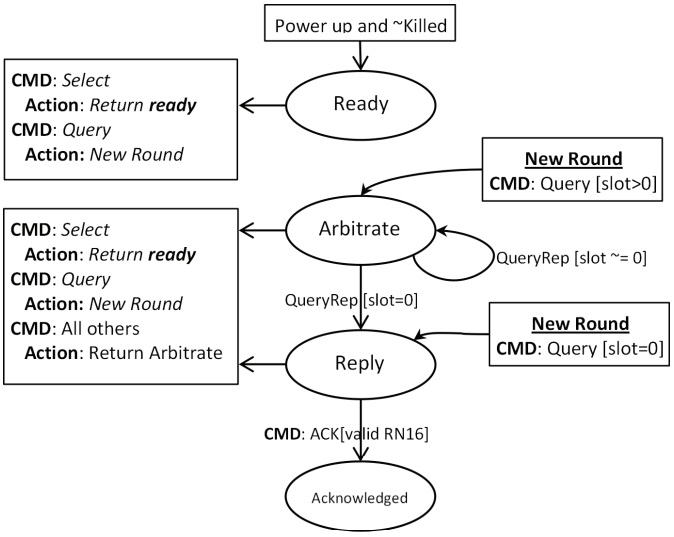

Fig. 7. EPC MAC algorithm running in transponders [1].

to backscatter its RN16 as shown in Fig. 8. Following the Query/QueryRep command, the reader transmits unmodulated carrier, CW(Continuous Wave), and listens to the tag replies. Assuming that a single tag replies, the reader acknowledges by sending ACK including the recently received RN16. Each of the tags decodes the ACK; if the included RN16 matches its own RN16 it responds by transmitting XPC/EPC packets. Therefore, in order for an inventory round to be *successful*, following conditions are necessary:

- Exactly one tag backscatters in response to Query / QueryRep command
- The transmitted RN16 from tag to reader is decoded error-free by the reader
- The XPC/EPC packet sent by the tag is decoded perfectly by the reader

Assuming three conditions above are met, a *Successful round* of length T_{SF} happens. Otherwise, failure on any of the conditions results in following *Unsuccessful rounds*:

- *Empty round*: An empty inventory round occurs if no tag responds back to Query/QueryRep. In this case, reader does not receive any RN16 and therefore no ACK is generated. Duration of this inventory round T_{Emp} is much shorter than T_{SF}.
- *Collided round*: Multiple transmission of RN16 results in collision. Assuming that reader detects the collision, no ACK is sent and a collided round of length T_{Cls} occurs. Readers utilize the reflected power or signal constellation analysis for detection of collision and may sometimes miss such a collision. If such a case, the reader continues by acknowledging the incorrectly decoded RN16 which results in a longer broken round, *invalid ACK*.
- *Invalid ACK round*: Erroneous decoding of RN16 by the reader leads to incorrect acknowledgment and eventually no XPC/EPC response is received from the tags. There are two situations which could result in *invalid ACK* replies - a) single tag replies with error in transmission of RN16 or b) multiple tags reply but reader does not detect collision. Duration of invalid ACK round T_{IA} is more than T_{Cls}, T_{Emp} but still less than T_{SF}.

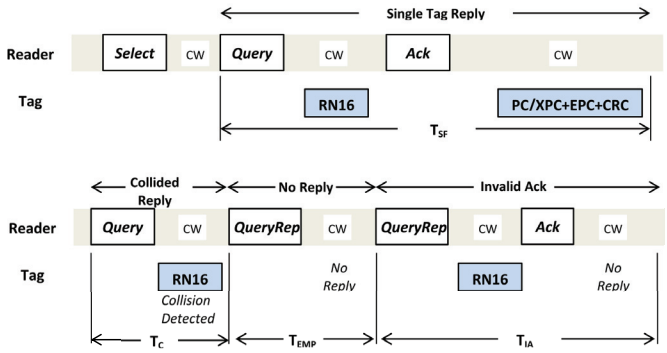

Fig. 8. EPC successful/unsuccessful inventory rounds.

Given a set of M tags in the vicinity of a reader, the probability of a *successful* inventory round in response to one Query command is

$$P_{SF} = \frac{M}{2^Q}\left(1-\frac{1}{2^Q}\right)^{M-1}(1-P_{e,RN}) \tag{15}$$

where $P_{e,RN}$ is probability of error in transmission of RN16. Here we have not considered error rate in XPC/EPC packet because it does not change the total length of the inventory round but it will be included later during performance analysis.

Probability of *empty* slot is

$$P_{Emp} = \left(1-\frac{1}{2^Q}\right)^{M} \tag{16}$$

and *collided* slot,

$$P_{Cls} = \left(1-P_{Emp}-\frac{M}{2^Q}\left(1-\frac{1}{2^Q}\right)^{M-1}\right)P_{cd} \tag{17}$$

where P_{cd} is the probability of collision detection by the reader given that collision has actually occurred. As mentioned before, P_{cd} depends on specific algorithm adopted by the reader for collision detection. Here, we do not confine our analysis to a specific algorithm and assume that reader always detects a collision whenever interfering transponders transmit different RN16 numbers (although they already have the same Q-bit slot counter, the remaining 16-Q bits of RN16 are assumed to be different) which results in $P_{cd} = 1-2^{-(16-Q)}$.

Based on previous discussion of the two scenarios leading to incorrect decoding of RN16, the probability of *invalid ACK* round is

$$P_{IA} = \frac{P_{Cls}\,(1-P_{cd})}{P_{cd}} + \frac{P_{SF}P_{e,RN}}{1-P_{e,RN}} \tag{18}$$

It is proven in [21] that the modulation and line coding techniques used in the EPC protocol is equivalent to a convolutional encoder of rate $R_c = 1/2$ with $d_{free} = 2$. Hence, probability of bit error, P_b, given that fading coefficients are known, can be approximated as below, in terms of symbol energy E received at the reader,

$$P_b \approx Q\left(\sqrt{2d_{free}R_cE/N_0}\right) = Q(\sqrt{2E/N_0}) \tag{19}$$

$$E = \left(\frac{\lambda}{4\pi r}\right)^4 \left(\frac{G_T G_R L_P}{2}\right)^2 \frac{\gamma_R \gamma_T P_T}{\text{UL rate}} \tag{20}$$

$$Q(s) = \frac{1}{\sqrt{2\pi}} \int_s^\infty e^{-\nu^2/2} d\nu \tag{21}$$

where γ_T and γ_R are tag-to-reader and reader-to-tag fading coefficient, respectively. The average probability of bit error $\overline{P_b}$ is calculated by averaging over both fading coefficients γ_T and γ_R. Considering a slow fading channel with Rayleigh distribution for both uplink and down link, the fading coefficients γ_T and γ_R will be exponentially distributed (squared Rayleigh random variables) with mean μ_T and μ_R, respectively. Therefore

$$\overline{P_b} \approx \int_0^\infty \int_0^\infty e^{-\frac{\gamma_T}{\mu_T} - \frac{\gamma_R}{\mu_R}} Q\left(\left(\frac{\lambda}{4\pi r}\right)^2 \frac{G_T G_R L_P}{2} \sqrt{\frac{2\gamma_T \gamma_R P_T}{(\text{UL rate}) N_0}}\right) d\gamma_T d\gamma_R \tag{22}$$

and probability of error while transmission of RN16 is

$$P_{e,RN} \approx 1 - \left(1 - \overline{P_b}\right)^{16} \tag{23}$$

One effective parameter in MAC layer calculations is tag population M. Precise estimation of M results in higher reading performance by increasing successful frame rate P_{SF} via balancing empty slot rate P_{Emp} against collision rate P_{Cls}. Various methods have been introduced for this purpose. Schoute [22] assumed a Poisson distribution for contending tags and estimated M in terms of the average of Poisson random variable. Vogt [8] improved population estimation strategy by using statistics of empty slots as well. Kodialam [23] proposed a new population estimation technique based on central limit theorem that is when the number of tags are large enough. Using this, one may achieve both estimation accuracy as well as the max-likelihood tag population [2].

Another approach is iterative algorithms such as Q algorithm in EPCglobal standards [1]. They modify the Q parameter in every iteration based on the results of last query round with the purpose of maximizing throughput (successful frames). If no tag replies during the last time slot, it decreases Q with a fixed rate to shrink the frame size (to decrease P_{Emp}). Otherwise, if collision occurs it increases Q to extend the frame size (lower P_{Cls}). Obviously, it will keep Q fixed if query is successful.

Furthermore, there are distributed approaches [24], [25] within which a rough estimation of the tag population is assumed available in a statistical from. The new strategy is to update the population distribution by Bayesian method based on tags' replies. The optimization is therefore to maximize the statistical average tag read rate. This method can track the value of M more accurately with the expense of higher complexity.

V. Performance Analysis

Maximizing the number of tags read within unit time or TRR(Tag Read Rate) is the metric of performance evaluation. TRR is a function of a number of system parameters including but not limited to M, Q, $T_{\text{on}}/T_{\text{off}}$ and link budget parameters r and P_T. In this section, we derive analytical results of TRR using energy model provided in Section II. Two approaches are considered for performance evaluations. First, *exact evaluation* of TRR with a focus on energy harvesting cycles is considered and second, the *asymptotic TRR*, sufficiently large T_{on}, is derived.

A. Exact Analysis

Assume a set of M tags in the vicinity of a reader, all at similar distances from the reader. We assume reader has a reasonable estimate of M based on which it sets up its MAC layer parameters such as Q. The energy harvesting cycle for every tag is $T = T_{\text{on}} + T_{\text{off}}$ given by (10)-(14). We seek to derive the expected number of *successful* inventories over an on-interval of length T_{on}.

Let $x(t)$ be the random number of successful queries in an interval of length t with expected value $X(t) = E\{x(t)\}$. Finding $X(t)$ includes considering all possible combinations of successful/unsuccessful rounds over t which is cumbersome. By the rule of iterated expectation, conditioning on the results of the first query round, we have

$$\begin{aligned} X(t) =& E\{x(t)\} \\ =& E\{x(t)|\text{success}\}P_{SF} + E\{x(t)|\text{empty}\}P_{Emp} \\ &+ E\{x(t)|\text{Inv. ACK}\}P_{IA} + E\{x(t)|\text{collision}\}P_{Cls} \\ =& [X(t - T_{SF}) + u(t - T_{SF})]P_{SF} + X(t - T_{IA})P_{IA} \\ &+ X(t - T_{Emp})P_{Emp} + X(t - T_{Cls})P_{Cls} \end{aligned} \tag{24}$$

Obviously $X(t) = 0$ for $\forall t < T_{SF}$, duration of one successful inventory round, which justifies the step function $u(t - T_{SF})$ above. Applying the Laplace transform to the above and simplifying,

$$\begin{aligned} X(s) =& P_{SF}\left[\frac{e^{-sT_{SF}}}{s} + e^{-sT_{SF}}X(s)\right] + P_{IA}e^{-sT_{IA}}X(s) \\ &+ P_{Emp}e^{-sT_{Emp}}X(s) + P_{Cls}e^{-sT_{Cls}}X(s) \\ =& \frac{e^{-sT_{SF}}P_{SF}}{s} \sum_{i=0}^{\infty} \left(P_{SF}e^{-sT_{SF}} + P_{Emp}e^{-sT_{Emp}} \right. \\ &\left. + P_{IA}e^{-sT_{IA}} + P_{Cls}e^{-sT_{Cls}}\right)^i \end{aligned} \tag{25}$$

Taking the Laplace inverse of (25) results in:

$$\begin{aligned} X(t) = P_{SF}u(t - T_{SF}) * \sum_{i=0}^{\infty} [P_{Emp}\delta(t - T_{Emp}) + \\ P_{Cls}\delta(t - T_{Cls}) + P_{IA}\delta(t - T_{IA}) + P_{SF}\delta(t - T_{SF})]^{(*i)} \end{aligned} \tag{26}$$

where $(*i)$ stands for i-fold convolution and could be simplified to

$$X(t) = P_{SF} \sum_{i,j,k,l} \frac{(i + j + k + l)!}{i!j!k!l!} P_{SF}^i P_{Emp}^j P_{IA}^k P_{Cls}^l \tag{27}$$

where summation is over $\forall i, j, k, l \in \{0, 1, ...\}$ such that $iT_{SF} + jT_{Emp} + kT_{IA} + lT_{Cls} \leq t - T_{SF}$. Equation (27) does not consider EPC packet loss in *successful* inventory rounds that is a result of channel noise. This could be considered by introducing a factor of $1 - P_{e,EPC}$ in the above calculation

where $P_{e,EPC}$ is probability of error in sending XPC/EPC packet of length 128 bits, given by (29).

$$X(t) = (1 - P_{e,EPC}) \sum_{i=0}^{n_S} \sum_{j=0}^{n_E} \sum_{k=0}^{n_{IA}} \sum_{l=0}^{n_C} \frac{(i+j+k+l)!}{i!j!k!l!} P_{SF}^{i+1} P_{Emp}^{j} P_{IA}^{k} P_{Cls}^{l} \quad (28)$$

where $n_S = \lfloor \frac{t - T_{SF}}{T_{SF}} \rfloor$, $n_E = \lfloor \frac{t-(i+1)T_{SF}}{T_{Emp}} \rfloor$, $n_{IA} = \lfloor \frac{t-(i+1)T_{SF} - jT_{Emp}}{T_{IA}} \rfloor$ and $n_C = \lfloor \frac{t-(i+1)T_{SF} - jT_{Emp} - kT_{IA}}{T_{Cls}} \rfloor$.

$$P_{e,EPC} = 1 - \left(1 - \overline{P_b}\right)^{128} \quad (29)$$

Tag read rate (TRR) is defined in terms of expected number of successful rounds in a unit of time:

$$\text{TRR} = \frac{X(T_{\text{on}})}{T} = \rho \frac{X(T_{\text{on}})}{T_{\text{on}}} \quad (30)$$

where $\rho = \frac{T_{\text{on}}}{T_{\text{on}} + T_{\text{off}}}$ is the tag duty cycle.

B. Asymptotic Rate

Equation (28) provides an exact formula for TRR based on various parameters but it does not provide much insight or guidance for system optimization. More useful results are plausible given additional assumptions. The asymptotic rate is the read rate in the limit when $T_{\text{on}} \to \infty$. Note this assumption *does not* mean that tag is working continuously or $\rho = 1$. The duty cycle is still less than unity, $\rho = \frac{T_{\text{on}}}{T_{\text{on}} + T_{\text{off}}}$, but both T_{on} and T_{off} are very large compared to duration of successful inventory round, $T_{\text{on}} >> T_{SF}$.

Assume K is the total number of inventory rounds (successful or unsuccessful) over an interval of duration T_{on}. The expected number of successful/empty/collided/Invalid-ACK rounds are KP_{SF}, KP_{Emp}, KP_{Cls} and KP_{IA}, respectively. As K, T_{on} approach infinity, the following equality holds:

$$T_{\text{on}} = K(P_{SF}T_{SF} + P_{Emp}T_{Emp} + P_{IA}T_{IA} + P_{Cls}T_{Cls}) \quad (31)$$

The asymptotic rate is thus defined as:

$$\begin{aligned} \text{TRR}_{\text{inf}} &= (1 - P_{e,EPC})\rho \lim_{T_{\text{on}} \to \infty} \frac{KP_{SF}}{T_{\text{on}}} \\ &= \frac{(1 - P_{e,EPC})\rho P_{SF}}{P_{SF}T_{SF} + P_{Emp}T_{Emp} + P_{Cls}T_{Cls} + P_{IA}T_{IA}} \end{aligned} \quad (32)$$

It must be noted that in the above analysis, the down link(DL) channel is assumed perfect (no error while decoding reader messages by transponders) which is a reasonable assumption given the high downlink carrier power.

VI. Simulation Results

Simulation results are provided for both model verification and performance evaluation. The EPC G2 C1 MAC was implemented in MATLAB under the following conditions:

- Simulations were performed at the packet level in MATLAB. Command packets - *Select, Query* and *ACK* - are generated by the reader and broadcast to the tags. Each tag receives an independent copy of the packet which may be corrupted by noise. Each tag responds individually to the command based on its current status (*Active/Standby*) and command parameters. The tag responses, including RN16 and XPC/EPC packets, are super-imposed and sent back to the reader [26].
- Tag and reader state machine are implemented independently as shown in Figs. 6 and 7. Every tag has its own state machine and is simulated separately. Harvesting cycles is also considered for transponders and as a result,

TABLE I
Glossary

Symbol	Definition
P_T	Transmitted power by the reader
P_{in}	Input power at the front-end of the tag antenna
$P_{in,DC}$	Rectified input power, converted from P_{in}
η_{rect}	Power rectification efficiency, $P_{in,DC}/P_{in}$
P_{tag}	Tag dissipated power while running (no standby)
P_{leak}	Leakage power due to leakage current in capacitors
G_R, G_T, L_P	Reader/Tag antenna gain, polarization loss
f_c	Carrier frequency of the reader
T_c	Carrier period, $1/f_c$
λ	Carrier wavelength of the reader
r	Tag to reader distance
I_{leak}	The leakage current of harvester capacitors
I_{load}	Tag current consumption while active
R_{ant}, Z_{ant}	Tag antenna resistance/impedance
V_{OC}	Voltage amplitude at tag antenna eq. to P_{in}
V_{dc}	Steady-state rectified voltage of harvester
$V_{dc,\text{on}}(t)$	Transient response of rectified voltage in *active* mode
$V_{dc,\text{off}}(t)$	Transient response of rectified voltage in *standby*
V_H	High level voltage threshold, used by PMB
V_L	Low level voltage threshold, used by PMB
V_t	Turn on threshold voltage of rectifying diodes
N	Number of charge pump stages in Dickson circuit
C	Capacity of internal capacitors in charge pump
C_S	Capacity of storage capacitor
T_{off}	Tag standby interval (voltage restoration interval)
T_{on}	Tag life time (activity interval)
ρ	Tag duty cycle, $\frac{T_{\text{on}}}{T_{\text{on}} + T_{\text{off}}}$
M	Number of active tags in the vicinity of the reader
Q	MAC control parameter for ALOHA frame length
E	Energy of received backscattered symbols at the reader
P_b	Uplink bit error rate
$P_{e,RN}$	Prob. of error in decoding RN16 by the reader
$P_{e,EPC}$	Prob. of error in decoding XPC/EPC by the reader
P_{Cls}	Prob. of *Collided* query round
P_{SF}	Prob. of *Successful* query round
P_{IA}	Prob. of *Invalid ACK* query round
P_{Emp}	Prob. of *Empty* query round
P_{cd}	Prob. of collision detection by the reader
T_{Cls}	Duration of a collided query round
T_{SF}	Duration of a successful query round
T_{IA}	Duration of an invalid ACK query round
T_{Emp}	Duration of an empty query round
$X(t)$	Avg. number of *Successful* queries in an interval of length t
TRR	Tag read rate, $\frac{X(T_{\text{on}})}{T_{\text{on}} + T_{\text{off}}}$
TRR_{inf}	Asymptotic tag read rate as $T_{\text{on}} \to \infty$
γ_R	Reader-to-tag fading coefficient
γ_T	Tag-to-reader fading coefficient

the number of active tags is time-varying.

- Powered up tags are always able to decode the reader packets (no error in the downlink). On the other hand, uplink tag packets are corrupted by AWGN channel noise and inter-tag interference. No ISI is considered. We assume that the reader is able to detect all tag collisions, as long as they transmit different RN16 numbers. Slow fading is considered for both uplink and downlink channels with $\mu_R, \mu_T = 1$ (γ_T and γ_R are exponential random variables with unit mean).
- Hard-decision Viterbi decoding is used by the interrogator to decode tag packets.
- According to EPC, tag symbols could be coded as either FM0 or Miller. Here, Miller 4 is simulated.
- All tags are synchronized to interrogator Query commands.

Down link and Up link baud rate directly affect TRR since they change duration of four types of inventory rounds introduced in section IV. For the sake of simulation, we have acquired following parameters from an actual implemented RFID platform (WISP) [19].

- BLF[3] $= \frac{1}{\text{Pulse Period}}$ =250kHz
- Miller Order (MO): 4
- Tari: $24\mu s$
- EPC packet length: 128 bits
- UL rate (Miller): $\frac{\text{BLF}}{\text{MO}} = 62.5$ kbps
- DL rate = $\frac{2}{3\text{Tari}} = 27.8$ kbps
- RTcal = 3.0×Tari
- $T_{Cls} = \frac{Query}{\text{DL rate}} + \frac{\text{RN16}}{\text{BLF}} + \frac{10}{\text{BLF}} = 1.8$ms
- $T_{Emp} = \frac{Query}{\text{DL rate}} + \max(\text{RTcal}, \frac{10}{\text{BLF}}) = 1.1$ms
- $T_{IA} = \frac{Query+ACK}{\text{DL rate}} + \frac{\text{RN16}}{\text{UL rate}} + \max(\text{RTcal}, \frac{10}{\text{BLF}}) = 2.5$ms
- $T_{SF} = \frac{Query+ACK}{\text{DL rate}} + \frac{RN16+EPCdata}{\text{UL rate}} = 5.0$ms

A. Duration of T_{on}

A fundamental parameter in calculation of TRR is T_{on}. Fig. 9 presents TRR/ρ v.s. T_{on} for Q=4 and M=16/32 tags. The purpose of normalization is to provide a fair comparison by factoring out the dependence on ρ. The simulation and analysis (30) perfectly match and validates the model. Increasing T_{on} monotonically increases TRR, subject to asymptotic rate given by (32).

It is inferred from Fig. 9 that TRR could decrease if the ratio $\frac{T_{\text{on}}}{T_{SF}}$ is not large enough. Regardless of other parameters, this ratio should be at least in the order of $20 \sim 30$ to achieve performance close to limit (TRR_{inf}). Hence, as long as this criteria is met, TRR could be well approximated by (32). This figure also shows that average number of *successful* query rounds is not proportional to T_{on} specially when $\frac{T_{\text{on}}}{T_{SF}} \not< 20$; this is because when T_{on} is small, if none of the first few query rounds at the beginning of the 'on' interval is successful, the tag goes to standby mode soon and no successful round ever happens over T_{on}. This reduces effective number of successful rounds below (32).

The maximum possible TRR is achieved when no empty, collided or invalid ACK rounds occur. This ideal rate is therefore governed only by the duration of successful rounds $\text{TRR}_{\text{max}} = \frac{\rho}{T_{SF}}$. It is beneficial to compare this with the asymptotic rate in Fig. 9. For the current simulation results

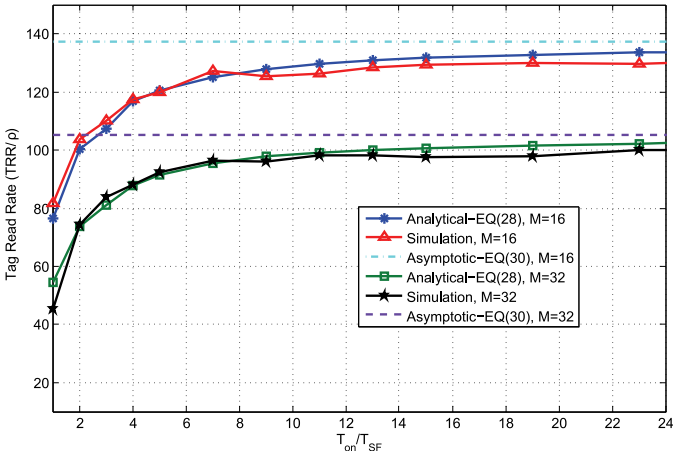

Fig. 9. Tag read rate, simulation and analytical results.

$\frac{\text{TRR}_{\text{max}}}{\rho} = 200$ and $\frac{\text{TRR}_{\text{inf}}}{\rho} = 137$ which reveals that the portion of rate reduction due to MAC deficiency is $\approx \%31.5$. Compared to traditional framed slotted ALOHA, this provide a more accurate result since collided and empty rounds in EPC are designed to have much lower durations than successful rounds.

B. TRR versus Q

Assuming that reader has an estimate of number of tags M, the parameter Q could be chosen accordingly to maximize TRR. General optimization with respect to Q implies setting $\frac{\partial \text{TRR}}{\partial Q} = 0$ where TRR is defined in (30). When $\frac{T_{\text{on}}}{T_{SF}} >> 1$, the simpler Eq. (32) may be used and optimum Q is set based on $\frac{\partial \text{TRR}_{\text{inf}}}{\partial Q} = 0$. For the latter case, the optimum Q_{opt} is found to be:

$$Q_{opt} = \log_2\left(1 + (M-1)\frac{T_{Cls}}{T_{Emp}}\right) \tag{33}$$

under two additional assumptions of $P_{e,RN} \approx 0$ (SNR is high at the reader) and $P_{cd} \approx 1$, collision is always detected by the reader. By considering traditional ALOHA based systems, where $T_{Cls} = T_{Emp}$, the optimum Q is $Q_{opt} = \log_2(M)$ which is in agreement with ALOHA literatures.

The role of Q parameter is to trade off between the average number of collided rounds versus empty rounds. If the length of a collided round, T_{Cls}, is larger than duration of an empty round, T_{Emp}, then it is obviously better to have more empty rounds instead of collided rounds in order to get the maximum TRR; this justifies the factor $\frac{T_{Cls}}{T_{Emp}}$ in (33).

Fig. 10 plots TRR as a function of Q for M=16/32 tags. Both simulation and analytical results (30) are shown to exactly match. The optimum Q for M=16 is $Q_{opt} = 4.6$ and for M=32, $Q_{opt} = 5.69$. However, based on EPC, only integer values are valid for Q and optimum values are found to be $Q_{opt,sim} = 4/5$ for M=16/32, respectively.

C. Evaluation of ρ

From (30), TRR is directly proportional to tag duty cycle ρ which in turn is a function of input power P_{in}, tag power P_{tag}, threshold voltages V_H, V_L and rectification efficiency

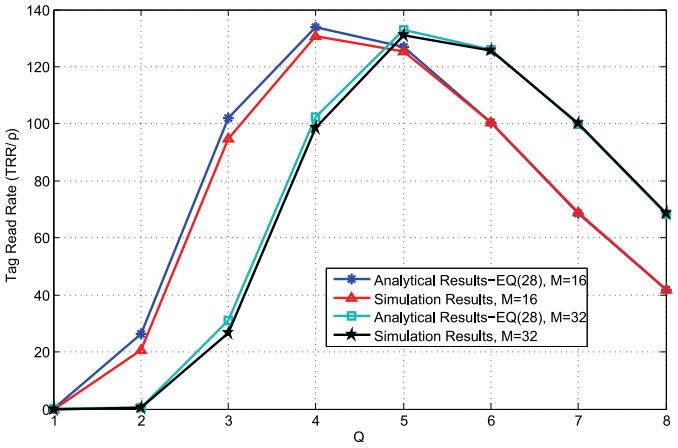

Fig. 10. Tag read rate as a function of Q, simulation and analytical results.

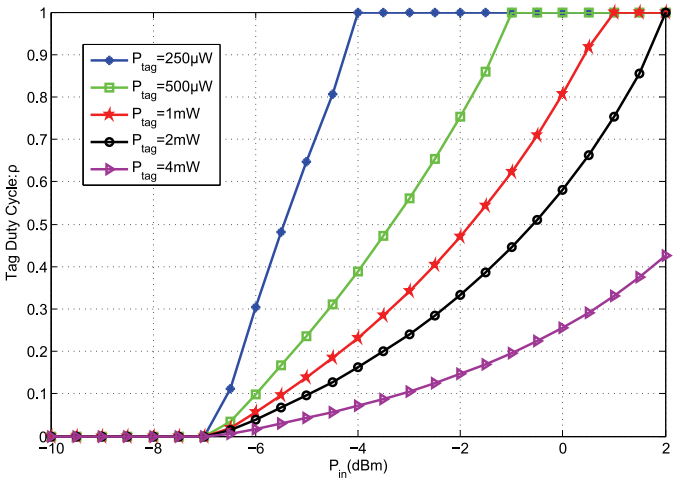

Fig. 11. Tag duty cycle versus P_{in} for various values of tag power P_{tag}.

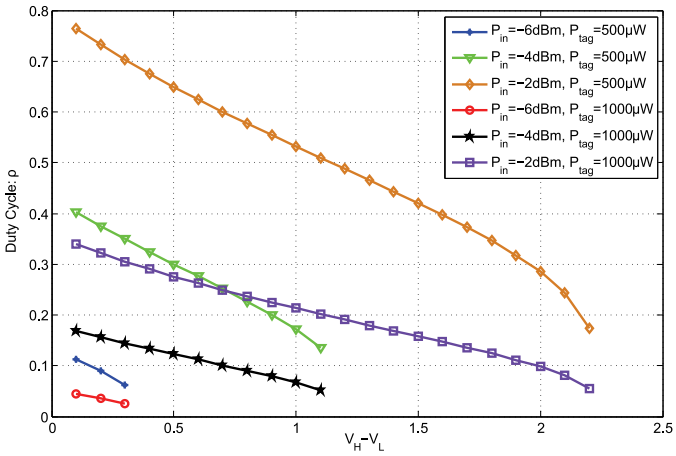

Fig. 12. Tag duty cycle, ρ, versus V_H for various combination of tag power, P_{tag}, and input power, P_{in}.

η_{rect}. Fig. 11 plots ρ as a function of P_{in} for four different values of P_{tag} and the following parameters:

- $R_{ant} = 50\Omega$
- $V_L = 1.8, V_H = 1.9, V_t = 0.1$
- $C_S = 10\mu F, C = 10pF$
- N=5
- $P_{leak} = 10\mu W$

It is inferred from the figure that the tag duty cycle is zero for $P_{in} \leq -7dBm$ regardless of P_{tag}. This is because maximum rectified voltage is less than V_L and tag never turns on. As P_{in} increases ρ also increases which in turn improves TRR from (30). The slope of increase is inversely proportional to P_{tag}. The duty cycle ρ reaches 1 when $\eta(V_L)P_{in} = P_{tag} + P_{leak}$ whereupon the tag stays active continuously. It is also inferred from Fig. 11 that decreasing tag power also increases ρ and pulls down the minimum required power for continuous activity of transponders.

Based on (14) duration of 'on' interval within each cycle, T_{on}, is a function of V_H. Therefore, increasing V_H is a possible way to increase T_{on} which is required to achieve asymptotic rate TRR_{inf} or to enable the tag accomplishes more time consuming operations. Increasing V_H has two major effects as

- *Operational Range*: Increasing V_H decreases maximum operational range because it pushes up the minimum required voltage which requires more input power or lower distance to the reader as in (4) by replacing V_L with V_H.
- *Duty Cycle* ρ: Changing V_H affects T_{on} and T_{off} in different non-linear ways. The resulting duty cycle ρ is therefore a function of V_H. This dependency is shown in Fig. 12 for various combinations of P_{in} and P_{tag}. Since V_H is limited to the maximum rectified voltage as in (8), increasing P_{in} extends the possible range of V_H. It is inferred from this figure that increasing V_H results in lower duty cycle ρ in all cases. The reason is clear, setting V_H closer to the $V_{\infty,\text{off}}$ increases T_{off} exponentially from (10) but it increases T_{on} almost linearly from (14).

D. TRR versus distance

Increasing distance has multiple effects on TRR, based on (32). First, it decreases duty cycle ρ if the effective rectified power $P_{in,DC}$ is less than required power P_{tag}. Second, it increases error probability in transmission of both RN16 and EPC data packet due to reduced SNR which in turn degrades probability of successful frame P_{SF}.

Fig. 13 shows overal TRR as a function of distance for a 4.0-Watt transmitter (EIRP=36 dBm) and for various values of P_{tag}. Regardless of how small is tag power P_{tag}, the maximum range is always limited to 4.5 meter. This is due to rectified voltage V_{dc} that drops below required minimum voltage V_L (1.8v in this case). The two effects of increased distance, as mentioned above, can be seen in this figure. In every case of P_{tag}, TRR drops fast at a certain distance ($d \geq 1$ for $P_{tag} = 2$mW, $d \geq 2$ for $P_{tag} = 500\mu$W) which is the point where harvested power falls below tag's required power and therefore duty cycling starts. Before reaching this point, TRR decreases at a slower rate due to SNR reduction (the effect of increased path loss as well as fading). This figure also displays TRR for a very low power tag ($P_{tag} \approx 0$) to bypass the effect of duty cycling on TRR. As can be seen, the decay rate is monotonically slow and solely due to reduced

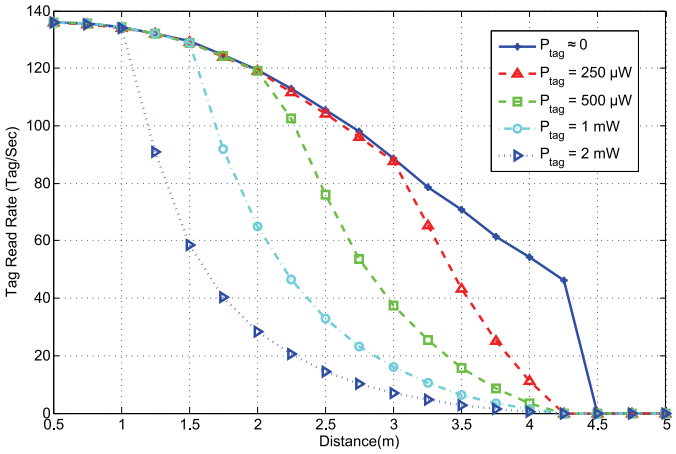

Fig. 13. Tag read rate, TRR, versus distance for various values of tag power, P_{tag}. The effect of fading is considered in simulation of both uplink and down link as exponentially distributed with unit average for γ_T,γ_R in (20).

SNR and higher $P_{e,RN}$ and $P_{e,EPC}$ which directly reduce TRR.

E. Comparison with Related Works

There have been a number of studies that attempts to either evaluate or improve MAC layer performance of EPC G2C1. For the purpose of comparison, some related simulation/implementation works are provided in this section. Based on Fig. 9 and for our simulation parameters (specially UL and DL rate), maximum achievable TRR is 130 tags/sec for unit duty cycle.

- In [9], empirical studies are provided using WISP with Alien reader (ALR-9800). Resulting TRR, provided for a high speed mode of DL = 128 kbps, UL = 250 kbps, M=16 tags and unit duty cycle ($\rho = 1$), is limited to 200 tag/sec. Since both DL and UL in this work are at least four times higher than our case (which translates to reduction of inventory round durations $T_{Cls}, ..., T_{SF}$ by 4) and based on (32), expected TRR is $4 \times \text{TRR}_{inf} \approx 4 \times 130 = 520$. The main reason for practical results being less than expectation is because of two power down periods (of length 40 ms and 3 ms) that Alien reader places between successive query super frames[4] and before CW[5] intervals and as a result it increases effective duration of inventory rounds or decreases TRR.
- In [27] the maximum rate of 1000 tag/sec is claimed which is reasonable because the uplink rate used was 640 kbps which is at least 10 times more than our case. Therefore at short ranges (where P_{in} is high enough to have $\rho = 1$) TRR values of $10 \times \text{TRR}_{inf} \approx 1300$ may be expected.
- In [28], TRR is presented as a function of UL/DL rates and for different anti-collision algorithms. For the case of EPC G2C1, Tari $= 25\mu s$ and UL=62.5kbps, TRR$\approx$ 190 which is higher than our results. This increase partly results from the EPC packet size in this work of 96 bits instead of 128 bits which decreases duration of T_{SF} from 5.0ms to 4.5ms.

[4]A series of query rounds that is used to inventory a tag population

[5]Continuous Wave, the interval of sending un-modulated carrier by the reader, used for receiving backscatter responses from tags

VII. Conclusion and Future Works

We introduced a new model for the stored energy in transponders that is based on tag energy harvesting structure, received power from reader and dissipated power by tag circuitry. This model describes how energy/voltage level is diminished while tag is active as well as the way it is restored back in standby mode. The results show that transient response of charge pump circuits is well approximated by a first order R-C circuit in both active and standby mode.

The proposed model was used for determination of maximum down link range within which rectified voltage is enough to turn on the transponder. The model also describes the duty cycling behavior of passive RFID systems and its main affecting factors. Analytical results were provided for duration of 'on'/'off' cycles in terms of tag circuit components as well as input/dissipated power. A general state machine for passive transponders and its effect on aforementioned energy model was presented. It includes reduction in input power because of carrier modulation by the reader and backscattering by the transponders.

The duty cycling as the main result of *Power Limitation* in RFID systems was considered together with *Tag Collisions* and *Link Failures* to evaluate the performance of passive RFID systems, specifically, the number of tags read in a unit of time by the reader. The resulting equations describes TRR as a function of various parameters such as P_{in}, P_{tag}, C_S, V_H/V_L, ... Under additional simplifying assumptions, asymptotic TRR was also presented which provides more intuitive results and can be used for system optimizations.

The energy is a major issue in passive RFID systems which should be carefully considered in EPC protocol. Current EPC standard does not consider transponder duty cycling and energy limitation. In our future work, we would like to propose a smarter MAC protocol that is based on provided energy model in this paper.

References

[1] EPC Radio-Frequency Identity Protocols Class-1 Generation-2 UHF RFID Protocol for Communication at 860 MHz-960 MHz, EPCglobal Std. 1.2.0, Oct. 2008.

[2] L. Zhu and T.-S. P. Yum, "Optimal framed aloha based anti-collision algorithms for RFID systems," *IEEE Trans. Commun.*, vol. 58, no. 12, pp. 3583–3592, 2010.

[3] Y. Cui and Y. Zhao, "Performance evaluation of a multi-branch tree algorithm in RFID," *IEEE Trans. Commun.*, vol. 58, no. 5, pp. 1356–1364, May 2010.

[4] C. Wang, M. Daneshmand, K. Sohraby, and B. Li, "Performance analysis of RFID generation-2 protocol," *IEEE Trans. Wireless Commun.*, vol. 8, no. 5, pp. 2592–2601, May 2009.

[5] Y.-C. Ko, S. Roy, J. R. Smith, H.-W. Lee, and C.-H. Cho, "RFID MAC performance evaluation based on ISO/IEC 18000-6 type c," *IEEE Commun. Lett.*, vol. 12, no. 6, pp. 426–428, 2008.

[6] J. Myung and W. L. J. Srivastava, "Adaptive binary splitting for efficient RFID tag anti-collision," *IEEE Commun. Lett.*, vol. 10, no. 3, pp. 144–146, 2006.

[7] Z. XIE and S. LAI, "Design and implementation of an active RFID MAC protocol," in *Proc. 2007 International Conference on Wireless Communications, Networking and Mobile Computing*, pp. 2113–2116.

[8] H. Vogt, "Efficient object identification with passive RFID tags," in *Proc. 2002 International Conference on Pervasive Computing*, pp. 98–113.

[9] M. Buettner and D. Wetherall, "An empirical study of UHF RFID performance," in *Proc. 2008 MobiCom*.

[10] X. Xu, L. Gu, J. Wang, G. Xing, and S.-C. Cheung, "Read more with less: an adaptive approach to energy-efficient RFID systems," *IEEE J. Sel. Areas Commun.*, vol. 29, no. 8, pp. 1684–1697, 2011.

[11] V. Namboodiri and L. Gao, "Energy-aware tag anticollision protocols for RFID systems," *IEEE Trans. Mobile Computing*, vol. 9, no. 1, pp. 44–59, 2009.

[12] P. J. Hawrylak, J. T. Cain, and M. H. Mickle, "Analytic modelling methodology for analysis of energy consumption for ISO 18000-7 RFID networks," *Int. J. Radio Frequency Identification Technol. and Applications*, vol. 1, no. 4, pp. 371–400, 2007.

[13] G. Bhanage and Y. Zhang, "Relay MAC: a collision free and power efficient reading protocol for active RFID tags," in *Proc. 2006 IEEE International Conf. on Computer Communications and Networks*, pp. 97–102.

[14] D. M. Dobkin, *The RF in RFID, Passive UHF RFID in Practice*. Elsevier, 2008.

[15] R. S. Wahby, "Radio frequency rectifiers for DC-DC power conversion," master's thesis, Massachusetts Institute of Technology, Cambridge, 2004.

[16] J. F. Dickson, "On-chip high-voltage generation in MNOS integrated circuits using an improved voltage multiplier technique," *IEEE J. Solid-State Circuits*, vol. 11, no. 3, p. 374378, Jun. 1976.

[17] R. E. Barnett, J. Liu, and S. Lazar, "A RF to DC voltage conversion model for multi-stage rectifiers in UHF RFID transponders," *IEEE J. Solid-State Circuits*, vol. 44, no. 2, pp. 354–370, 2009.

[18] G. D. Vita and G. Iannaccone, "Design criteria for the RF section of UHF and microwave passive RFID transponders," *IEEE Trans. Microwave Theory and Techniques*, vol. 53, no. 9, pp. 2978–2990, 2005.

[19] A. P. Sample, D. J. Yeager, P. S. Powledge, A. V. Mamishev, and J. R. Smith, "Design of an RFID-based battery-free programmable sensing platform," *IEEE Trans. Instrumentation and Measurement*, vol. 57, no. 11, pp. 2608–2615, 2008.

[20] F. Hessar (2011), PSPICE simulation of RF rectifier for RFID. Available: http://www.ee.washington.edu/research/funlab/archive.html

[21] M. Simon and D. Divsalar, "Some interesting observations for certain line codes with application to RFID," *IEEE Trans. Commun.*, vol. 54, no. 4, pp. 583–586, 2006.

[22] F. C. Schoute, "Dynamic frame length ALOHA," *IEEE Trans. Commun.*, vol. COM-31, no. 4, pp. 565–568, 1983.

[23] M. Kodialam and T. Nandagopal, "Fast and reliable estimation schemes in RFID systems," in *Proc. 2006 MobiCom*.

[24] C. Floerkemeier, "Transmission control scheme for RFID object identification," in *Proc. 2006 Pervasive Wireless Networking Workshop*.

[25] ——, "Bayesian transmission strategy for framed ALOHA based RFID protocols," in *2007 IEEE International Conf. RFID*.

[26] F. Hessar (2011), Energy based simulation of EPC G2C1 MAC Layer in MATLAB. Available: http://www.ee.washington.edu/research/funlab/archive.html

[27] (2008) Impinj - Speedway Reader documentation. Available: {http://www.impinj.com/Documents/Reader/Speedway_Reader_Brochure/}

[28] S. Roy, V. Jandhyala, J. R. Smith, D. J. Wetherall, B. P. Otis, R. Chakraborty, M. Buettner, D. J. Yeager, Y.-C. Ko, and A. P. Sample, "RFID: from supply chains to sensor nets," *IEEE Trans. Instrumentation and Measurement*, vol. 98, no. 9, pp. 1583–1592, 2010.

Farzad Hessar Farzad Hessar received the B.S. degree in Electrical Engineering from the Amirkabir University of Technology in 2008 and M.S. degree in Electrical Engineering from the Sharif University of Technology in 2010. Currently he is pursuing a Ph.D. degree in Electrical Engineering at the University of Washington. His current research interests include low power wireless communication and its application to RFID as well as Cognitive Radio Systems including TV White Space Spectrum. In the past, he has worked as Communication System Designer for various research labs and corporations.

Sumit Roy, Fellow IEEE Sumit Roy received the B. Tech. degree from the Indian Institute of Technology (Kanpur) in 1983, and the M. S. and Ph. D. degrees from the University of California (Santa Barbara), all in Electrical Engineering in 1985 and 1988 respectively, as well as an M. A. in Statistics and Applied Probability in 1988. Presently he is Professor of Electrical Engineering, Univ. of Washington where his research interests include analysis/design of wireless communication and sensor network systems with a diverse emphasis on various technologies: wireless LANs (802.11) and emerging 4G standards, multi-standard wireless inter-networking and cognitive radio platforms, vehicular and underwater networks, and sensor networking involving RFID technology.

He spent 2001-03 on academic leave at Intel Wireless Technology Lab as a Senior Researcher engaged in systems architecture and standards development for ultra-wideband systems (Wireless PANs) and next generation high-speed wireless LANs. During Jan.-July 2008, he was Science Foundation of Irelands E.T.S. Walton Awardee for a sabbatical at University College, Dublin and was the recipient of a Royal Acad. Engineering (UK) Distinguished Visiting Fellowship during summer 2011. His activities for the IEEE Communications Society (ComSoc) includes membership of several technical and conference program committees, notably the Technical Committee on Cognitive Networks. He currently serves on the Editorial Board for IEEE TRANSACTIONS COMMUNICATIONS and IEEE TRANSACTIONS ON INTELLIGENT TRANSPORTATION SYSTEMS. He was elevated to IEEE Fellow by Communications Society in 2007 for his "contributions to multi-user communications theory and cross-layer design of wireless networking standards".